



Effects of annealing process on sagging resistance of cold-rolled three-layer Al alloy clad sheets

Yuan-yuan ZHAO, Zhen-yan ZHANG, Li JIN, Jie DONG

National Engineering Research Center of Light Alloy Net Forming & State Key Laboratory of Metal Matrix Composites, Shanghai Jiao Tong University, Shanghai 200240, China

Received 8 October 2015; accepted 26 January 2016

Abstract: The effects of annealing process on the hardness, microstructure, Si diffusion, and the sagging resistance of cold-rolled 4343/3003/4343 Al alloy clad sheets and their 3003 Al alloy core sheets were experimentally investigated through hardness tests, EBSD observations, EDS analysis, and sagging test. The results showed that with the increase of annealing temperature, the hardness of both clad sheet and core sheet decreased, while the sagging resistances of both clad and core sheets achieved maximum values after annealing at 380 °C for 1 h. After annealing at 380 °C, the clad layer contained fine and equiaxed recrystallized grains; the core layer was composed of fully recrystallized coarse grains elongated along the rolling direction. The Si diffusion from the clad layer to the core zone was limited. After annealing at a higher temperature of 440 °C or 550 °C, the sagging resistance of clad sheets worsened precipitously. The grains in the clad layer grew up, obscuring the interface between the clad and core layer; the recrystallized grains in the core layer became finer. Significant amount of Si penetrated into the core layer through the accelerated diffusion. Compared with the microstructure refinement, Si diffusion is the main factor influencing the sagging resistance.

Key words: aluminum alloy; microstructure; annealing; Si diffusion; sagging resistance

1 Introduction

Multi-layer aluminum brazing sheets featuring low density, high thermal conductivity, and excellent corrosion resistance are becoming predominant for producing the fins of automotive heat exchangers [1,2]. Aluminum heat exchangers are generally produced by brazing aluminum brazing sheets and multiport Al tubes at 600 to 610 °C. The cold-rolled 4343/3003/4343 Al alloy clad sheets, with a clad/core layered structure, are the most widely used aluminum brazing materials for heat exchangers. The 4343 alloy clad layer made from an Al–Si hypo-eutectic alloy with a low melting point of 570–610 °C, completely melts and forms a brazed joint with multiport Al tube during brazing. The 3003 alloy core layer made from an Al–Mn alloy has a higher melting point of 630–650 °C and provides the structural rigidity during the high temperature brazing [3]. The ever stringent regulations of automotive fuel economy standards call for more aggressive mass reduction in vehicular components, including a thinner aluminum

brazing sheet [4,5]. This change will post a serious challenge for the manufacturing as the weaker heat exchanges may collapse during brazing [6].

To improve the high temperature mechanical strength of aluminum sheets, also termed sagging resistance, many studies have focused on the deformation mechanisms during brazing. Researchers suspected that the Si diffusion and microstructure were factors affecting the sagging resistance of the aluminum sheet. GAO et al [7] simulated the brazing process of aluminum sheets and confirmed the Si diffusion into the core layer by EPMA. TURRIFF et al [3] investigated the microstructure evolution induced by Si diffusion and observed the formation of coarse Al–Si eutectic phase during brazing. The research conducted by RYU et al [8] and NOH et al [9] indicated that Si content in the core alloy worsened the sagging resistance. It could be concluded that Si diffusion had a negative impact on the sagging resistance.

QIN et al [10] evaluated the brazability of an Al–Mn cold-rolled sheet and found that recrystallized coarse grains could reduce the grain boundary slip which

was beneficial to the sagging resistance. After investigating the microstructure evolution of three-layered aluminum brazing sheets, KIM et al [11] revealed that Si diffusion in the recrystallized coarse grains was reduced compared with that in a deformed microstructure. Besides, the coarse grains were less prone to grain erosion, which further improved collapse resistance [12–15]. Nevertheless, the exact reason of collapse during brazing is still unclear and there lacks systematic study in the literature. The current research aimed at addressing the influence of different annealing processes on the sagging resistance of 4343/3003/4343 aluminum clad sheets via microstructure evolution and Si diffusion. The sagging resistance of 3003 core sheets was compared with the 4343/3003/4343 clad sheets, so that a comprehensive understanding of the deformation mechanism in the brazing process can be established and the main factor affecting the sagging resistance can be revealed.

2 Experimental

The aluminum clad sheet was manufactured by Nantong Hengxiu Aluminum Heat Transfer Materials Co., Ltd., and consisted of an AA3003 core and an AA4343 clad on each side. The chemical compositions of the raw material are shown in Table 1. After hot-rolling and cold-rolling, the three-layer aluminum was reduced by over 99% to a thickness of 0.15 mm in the normal direction (ND) with a cladding ratio of 8% on each side. Because of high rolling reduction, the 4343/3003/4343 clad sheet contained heavily deformed grains elongated in the rolling direction (RD), which is hard to be confirmed by electron backscatter diffraction and optical microscopy.

Table 1 Chemical compositions of 4343/3003/4343 clad sheet

Sheet	Mass fraction						
	Si	Fe	Mn	Cu	Zn	Zr	Al
Core/3003+ 1.5%Zn	0.4	0.5	1.3	0.1	1.5	0.1	Bal.
Clad/4343	8.0	0.1	0.2	0.1	–	–	Bal.

To separate the effect of Si diffusion on the sagging resistance during brazing, the 4343/3003/4343 clad sheet was electropolished to remove the 4343 clad layer in a solution of 30% (volume fraction) nitric acid and methanol at $-30\text{ }^{\circ}\text{C}$ and 12 V. The electropolished specimen without Si diffusion was designated as 3003 core sheet, and the specimen without electrolytic polishing was referred to as 4343/3003/4343 clad sheet.

Both the 3003 core sheet and the 4343/3003/4343 clad sheet were annealed at 380, 440, 550 $^{\circ}\text{C}$ for 1, 2, 3 h, respectively, and then water-quenched to room temperature. After annealing, the hardness on the

RD–ND cross section of the samples was tested by an HX–500 microhardness tester. Since the hardness was measured in the core zone of 4343/3003/4343 clad sheet, the 4343 clad layers were removed by electrolytic polishing after annealing.

The cold-rolled 4343/3003/4343 clad sheet and the specimens annealed for 1 h at various temperatures were held at 610 $^{\circ}\text{C}$ for 10 min to simulate the brazing process. The samples were cut into rectangle specimens of 90 mm long and 30 mm wide, whose length direction is parallel to the RD. The schematic of the sagging test is shown in Fig. 1. One end of the specimen was fixed and the other end of 50 mm long was free. The sagging distance was defined as the deflection of the free end after brazing. The sagging test was performed in a heating furnace, which had been held at 610 $^{\circ}\text{C}$ for 20 min to diminish temperature variation.

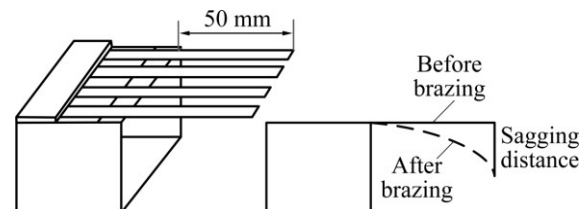


Fig. 1 Schematic view of sagging test rig

A set of microscopy techniques were used to characterize the microstructure evolution of both 4343/3003/4343 clad sheet and 3003 core sheet after annealing and brazing (sagging test). Samples were ground mechanically and polished in a 1 μm diamond polish. Etching was carried out by immersing samples in a 0.5% HF solution for 60 s. Then, the microstructures on the RD–ND cross sections of different aluminum clad sheets were observed by optical microscope (OM) and scanning electron microscope (SEM) QUANTA FEG–250. Electron backscatter diffraction (EBSD) was used to quantify the grain size after annealing and brazing. The Si diffusion before and after brazing was monitored by energy dispersive spectrometer (EDS). To observe the fine precipitated particles, the samples were twin-jet electropolished (at $-20\text{ }^{\circ}\text{C}$, 15 V) with a solution of 33% HNO_3 in methanol and observed under a transmission electron microscope (TEM).

3 Experimental results

3.1 Hardness of annealing clad sheets and core sheets

Figure 2 exhibits the Vickers microhardness of 4343/3003/4343 clad sheet and 3003 core sheet as a function of annealing temperature and annealing time. Both specimens displayed similar trend of hardness evolution. The hardness of cold-rolled clad sheet was HV 93.8. After annealing, the hardness values of

4343/3003/4343 clad sheet and 3003 core sheet were respectively reduced to HV 51.2 and HV 50.9 after annealing at 380 °C for 1 h. Extending the annealing temperature above 380 °C or annealing time beyond 1 h only marginally decreased the hardness, indicating that the aluminum sheet has fully recrystallized.

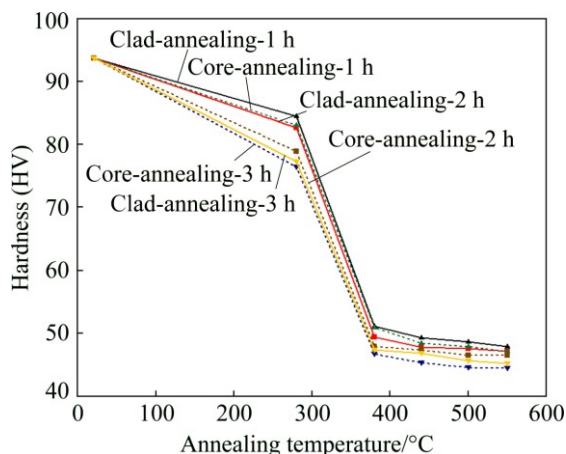


Fig. 2 Hardness of 4343/3003/4343 clad sheet and 3003 core sheet after different annealing processes

Under the same annealing condition, 4343/3003/4343 clad sheet exhibited a little higher microhardness values than 3003 core sheet, which may be attributed to the solid solution hardening from Si permeation into the core zone during annealing [16].

3.2 Microstructure evolution of annealing clad sheets and core sheets

In deformed and supersaturated Al–Mn alloys, precipitation occurs before or simultaneously with recovery and recrystallization (referred to as concurrent precipitation) [17]. The effect of concurrent precipitation depends on the critical temperature (TC), which varies in the range from 300 to 450 °C depending on the level of Mn supersaturation. At temperature below TC, concurrent precipitation tends to retard recovery and recrystallization, and results in the formation of large and pancake-like grains. At temperature greater than TC, recrystallization is only slightly affected by concurrent precipitation, leading to fine and equiaxed grains [18–21].

As shown in Fig. 2, 4343/3003/4343 clad sheet has been fully softened after annealing at 380 °C or higher temperature for 1 h. These specimens were chosen to study the microstructure evolution. Figures 3 displays the microstructure evolution of 4343 alloy clad layer and 3003 alloy core layer annealed at various temperatures. The cold-rolled 4343/3003/4343 clad sheet annealed at 380 °C for 1 h shows a three-layer sandwich structure. The clad layer consists of fine and equiaxed grains, while

the core layer is composed of fully recrystallized coarse grains that are elongated along the rolling direction. According to the theory of concurrent precipitation, Mn-bearing dispersoids precipitate before recrystallization and subsequently suppress the nucleation of recrystallization when the annealing temperature is below TC. This leads to inhomogeneous and coarse grain structure [22]. Moreover, the precipitation occurs preferentially at the high angle grain boundaries aligned in the RD and hence inhibits the grain growth in the ND due to the large Zener drag [23,24]. With the extension of annealing time, the grains in the clad layer grow up gradually, but the interface remains distinguishable between the dramatically different microstructures of the clad and core layers (shown in Fig. 3(a)). The size of coarse grains in the core layer does not change much, which is probably due to the Zener pinning of the dispersoids formed during concurrent precipitation.

When annealed at 440 °C for 1 h, the microstructure in the clad layer was also fully recrystallized with equiaxed grains larger than that annealed at 380 °C. Recrystallization and precipitation happened simultaneously, yielding a complex microstructure in the core layer. A larger number of fine recrystallized grains were found within the coarse and pancake-like grains or at the grain boundary, as higher annealing temperature provided more energy for recrystallization nucleation in the deformed zone around the coarse intermetallic particles [25]. With the increased annealing time, fine grains in the clad layer grew up and coarse grains with higher surface energy in the core layer grew into the clad layer, resulting in an obscure and rugged interface between the core and clad layers (shown in Fig. 3(b)). The microstructure in the core layer remained identical except that the fine recrystallized grains within the coarse grains or at the grain boundary grew up gradually with the extended holding time.

When increasing the annealing temperature to 550 °C, the grains in the clad layer were much larger than those annealed at lower temperatures and the interface became fuzzy quickly due to epitaxial grain growth in the core layer. At 550 °C, the recrystallization in the core layer was completed within several seconds, long before precipitation occurred, so concurrent precipitation of dispersoids has less effect on recrystallization behavior [26]. Consequently, the fine dispersoids in the core zone retarded the grain growth and reduced the average grain size [27]. As summarized in Table 2, the higher the annealing temperature is, the smaller the average grain size is. When annealed at 550 °C for longer time, the fine and equiaxed grains in the core zone gradually grew up and the microstructure became more homogenous.

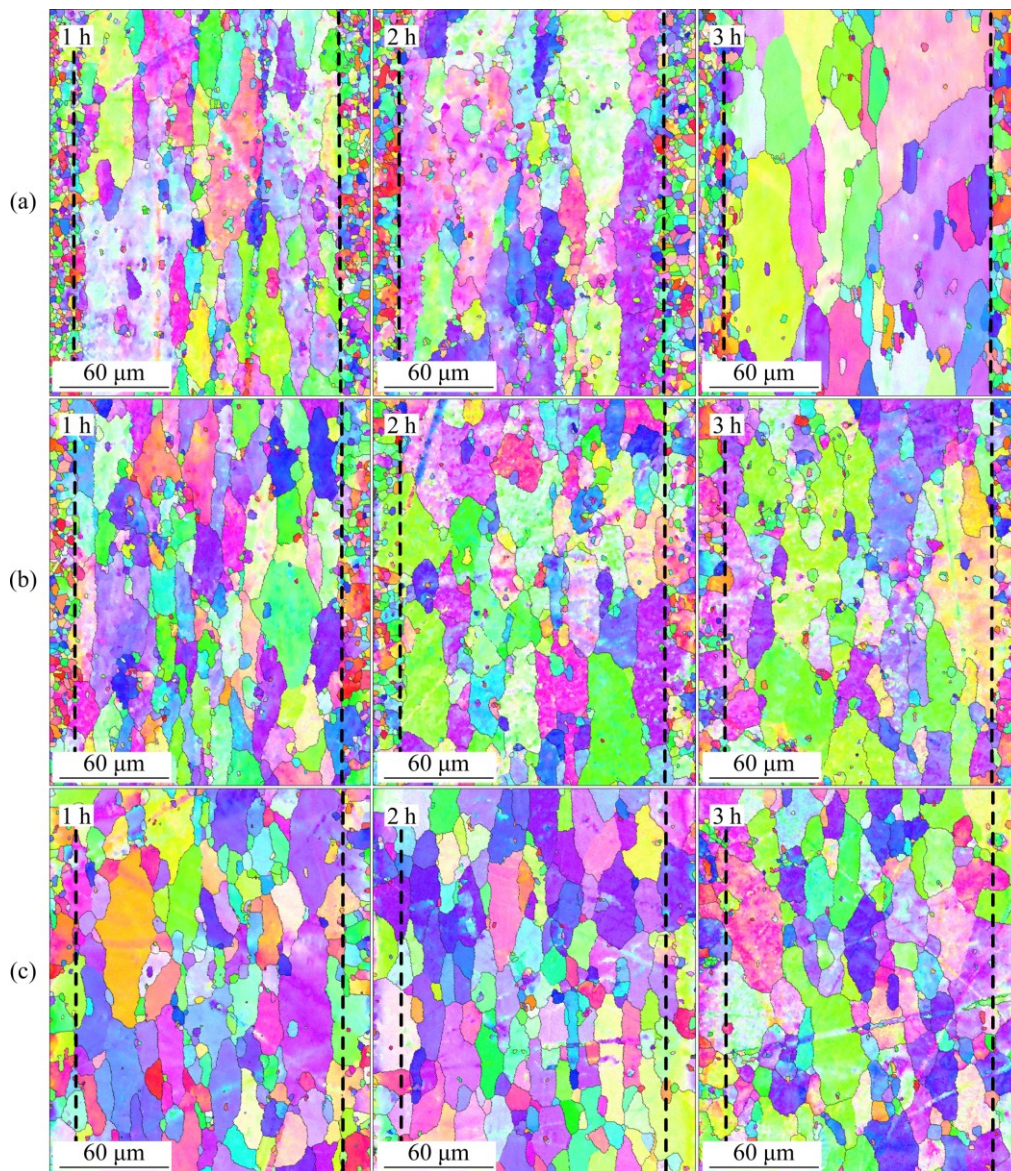


Fig. 3 Microstructure evolution of 4343/3003/4343 clad sheet after different annealing processes (black dotted lines mark interfaces between clad layer and core layer) annealed at different temperatures: (a) 380 °C; (b) 440 °C; (c) 550 °C

Table 2 Grain size of 4343/3003/4343 clad sheet and 3003 core sheet after annealed for 1 h and after brazing

Annealing process	Average grain size after annealing/ μm	Average grain size after brazing/ μm
Clad-380 °C	36.5	48
Core-380 °C	29.5	42.7
Clad-440 °C	26.6	34
Core-440 °C	22.4	24.9
Clad-550 °C	22.7	22.9
Core-550 °C	20.2	19.9

The microstructure evolution of 3003 core sheet after 1 h annealing test is illustrated in Fig. 4. According to the hardness diagram, the 3003 core sheet is soft and

fully recrystallized at an annealing temperature above 380 °C. The microstructure is similar to that of the core zone of the 4343/3003/4343 clad sheet, and pancake shaped grains were observed. After annealing at 440 and 550 °C, the effect of concurrent precipitation is weakened and the recrystallization nucleation is added. Hence, the number of fine and equiaxed grains increased in the 3003 core sheet and the average grain size became smaller (referring to Table 2).

3.3 Si distribution in annealed clad sheets

As for the cold-rolled 4343/3003/4343 clad sheet, the Si content in the clad layer is 7.5% (mass fraction), much higher than that in the core layer, and the Si element in the clad diffused into the core during high temperature annealing [28]. The Si element distribution

on the cross section of annealed 4343/3003/4343 clad sheet has been measured by the EDS line scan, as presented in Figs. 5(a₁)–(a₃). And the distributions of Al element (in green lines) and other elements such as Mn, Cu, Fe and Zn are shown in Figs. 5(b₁)–(b₃).

After annealing at 380 °C for 1 h, the Si content in both clad layers was much higher than that in the core zone, indicating that there was little Si penetration into the core zone. Raising the annealing temperature to 440 °C or 550 °C increased solid-state diffusion of Si

from the clad to the core layer and substantially enhanced the Si concentration in the core layer [29].

3.4 Sagging resistance of annealed clad sheets and core sheets

Since annealing time has less impact on the microstructure and hardness of the clad sheets, the specimens annealed for 1 h were chosen for studying the sagging resistance.

Figure 6 displays the sagging distance of annealed

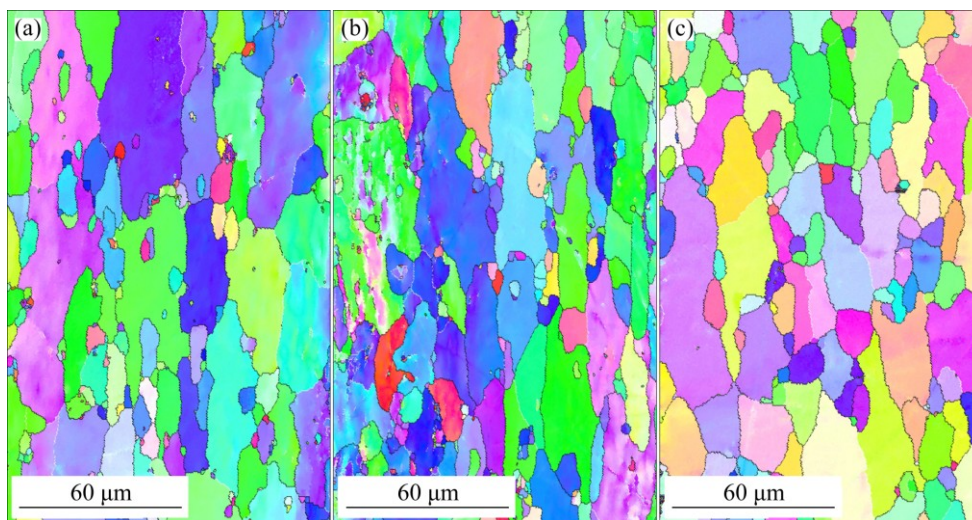


Fig. 4 Microstructure evolution of 3003 core sheet after annealing for 1 h at different temperatures: (a) 380 °C; (b) 440 °C; (c) 550 °C

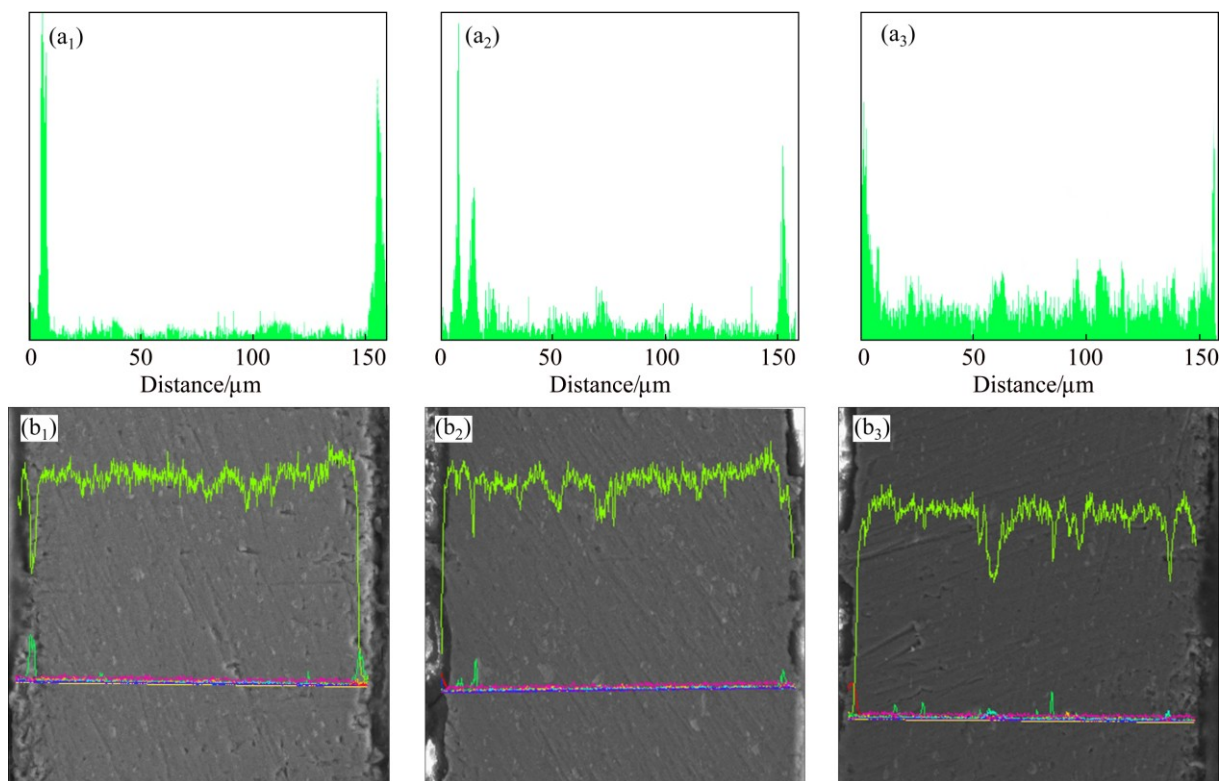


Fig. 5 Si element distribution across interface of 4343/3003/4343 clad sheet after different annealing processes: (a₁, b₁) 380 °C for 1 h; (a₂, b₂) 440 °C for 1 h; (a₃, b₃) 550 °C for 1 h

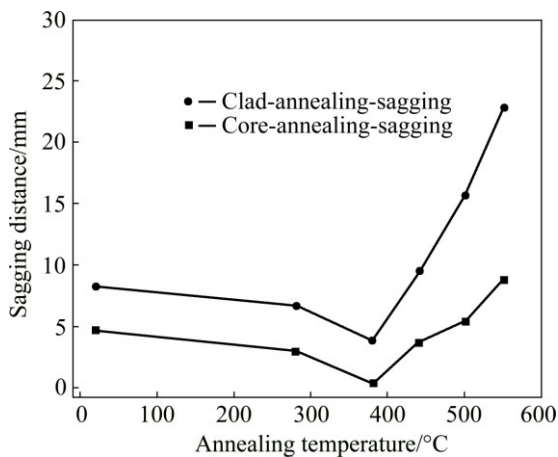


Fig. 6 Sagging distance after brazing of annealed 4343/3003/4343 clad sheet and 3003 core sheet

4343/3003/4343 clad sheet and 3003 core sheet. The sagging distance evolutions of clad and core sheets are similar: both decrease at first and then increase rapidly with the rise of annealing temperature. The 4343/3003/4343 clad sheet and 3003 core sheet annealed at

380 °C for 1 h exhibit better sagging resistance than specimens annealed in other conditions and the as-rolled specimen. Thus, it indicates that proper annealing process can improve the sagging resistance of the cold-rolled clad sheet. As shown in Fig. 6, the sagging distance of 3003 core sheet is less than that of 4343/3003/4343 clad sheet, suggesting that the clad layer adversely affects the sagging resistance. Besides, the sagging distance of clad sheet increases much more rapidly than the core sheet with the elevated annealing temperature.

4 Discussion

4.1 Effect of grain sizes of annealed clad sheets on sagging resistance

As shown in Fig. 7, after high temperature brazing, there is an obvious distinction between the microstructure evolutions of specimens under different annealing conditions. Both the clad sheet and core sheet annealed at 380 °C for 1 h showed coarse and elongated grains, indicating rapid grain growth during brazing.

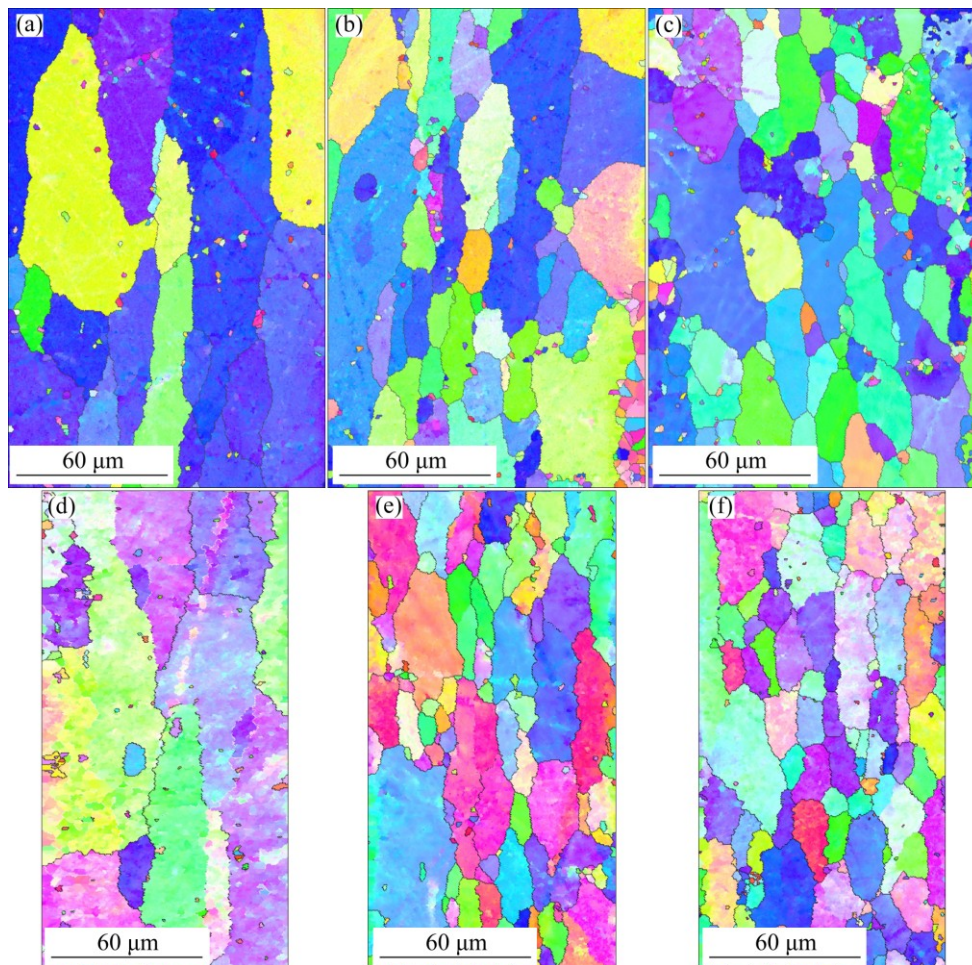


Fig. 7 Microstructures after brazing (sagging test) for 4343/3003/4343 clad sheet and 3003 core sheet under different annealing conditions: (a) Clad, 380 °C for 1 h; (b) Clad, 440 °C for 1 h; (c) Clad, 550 °C for 1 h; (d) Core, 380 °C for 1 h; (e) Core, 440 °C for 1 h; (f) Core, 550 °C for 1 h

Upon increasing the annealing temperature to 440 °C, the grains grew up slightly during brazing, while the specimens annealed at 550 °C exhibited almost identical grain size before and after brazing, indicating that grains did not grow up during brazing (shown in Table 2).

The specimens annealed at 380 °C for 1 h exhibited the best sagging resistance because coarse grains with reduced grain boundary areas were able to reduce the grain boundary sliding, enhancing the mechanical strength during brazing. According to SUZUKI et al [30], the fully recrystallized core alloy with coarse and anisotropic grains will provide stability to the interface between the core and clad layers, which improves the sagging resistance. In addition, the elongated coarse grain due to concurrent precipitation can also retard the Si diffusion into the core layer. However, further increasing the annealing temperature did not cause grain growth during brazing but accelerated grain boundary slip, degrading the sagging resistance.

After brazing, the specimens under different annealing conditions show entirely different microstructures, which might be related to different precipitation behaviors during annealing. Figures 8(a) and (b) exhibit the TEM images of dispersoids precipitation after annealing. Due to the low diffusion rate of Mn, Mn-enriched dispersoids could only nucleate in local areas with highly enriched Mn [31]. As a result, at low annealing temperatures, such as 380 °C, only scattered dispersoids (probably the unstable $Al_6(FeMn)$ particles) were observed [32]. When brazing at 610 °C, the Zener pinning of the scattered dispersoids was too weak to hinder the migration of grain boundaries. Therefore, the grains grew up rapidly as shown in Figs. 7(a) and (d). In contrast, a large number of dispersed particles less than 1 μm precipitated at 550 °C, as shown in Fig. 8(b). Most of the black dispersoids are believed to be stable $\alpha-AlMnFeSi$ particles [33]. These fine dispersoids suppressed the grain growth during annealing as well as after brazing. Large grain size was preferred for excellent sagging resistance by reducing grain boundary slip and Si penetration. As a result, the sheets annealed at 380 °C exhibited the best sagging resistance while that annealed at 550 °C exhibited the worst sagging resistance.

4.2 Effect of Si diffusion in annealed clad sheets on sagging resistance

During the brazing process, Si elements in the partially melt clad will penetrate into the core alloy. As shown in Fig. 9, there was much more Si diffusing into the core layer after brazing, compared with the annealed clad sheet shown in Fig. 5. After high temperature brazing, the Si element distribution in the clad layers was much higher than that of the core layer in the clad sheet

annealed at 380 °C. The difference in Si concentration was narrowed when the annealing temperature reached 440 °C. It became almost uniform throughout the clad and core layers in clad sheet annealed at 550 °C.

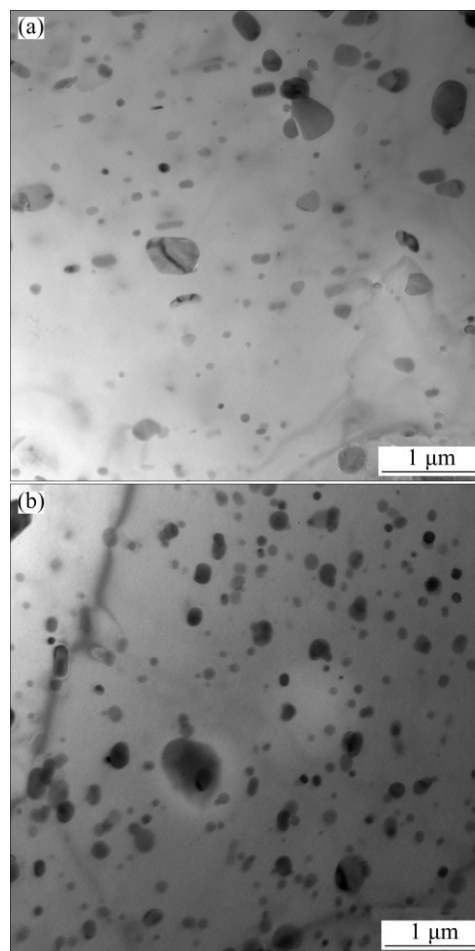


Fig. 8 TEM images of precipitates for 4343/3003/4343 clad sheet after annealing for 1 h: (a) 380 °C; (b) 550 °C

Since the melting temperature of Al–Si eutectic phase is 577 °C, much lower than that of the 3003 core sheet, the diffusion of Si into the core during brazing will lower the solidus temperature [34] and consequently weakens the high-temperature strength. In the polycrystal, the diffusivity is much higher in the grain boundary regions than in the bulk material [35]. This is especially for the case of the high-angle grain boundary which is the preferred pathway for Si diffusion during brazing. This implies a positive correlation between the area of grain boundary and the extent of Si diffusion. Compared with the as-rolled sheet, coarse grains developed at 380 °C weakened the Si diffusion during brazing. Besides, recrystallized grains elongated along the RD also restricted the Si penetration. Increasing the annealing temperature to 440 °C or higher significantly reduced the average grain size. Such an abnormal grain refinement offered additional pathways to the enhanced

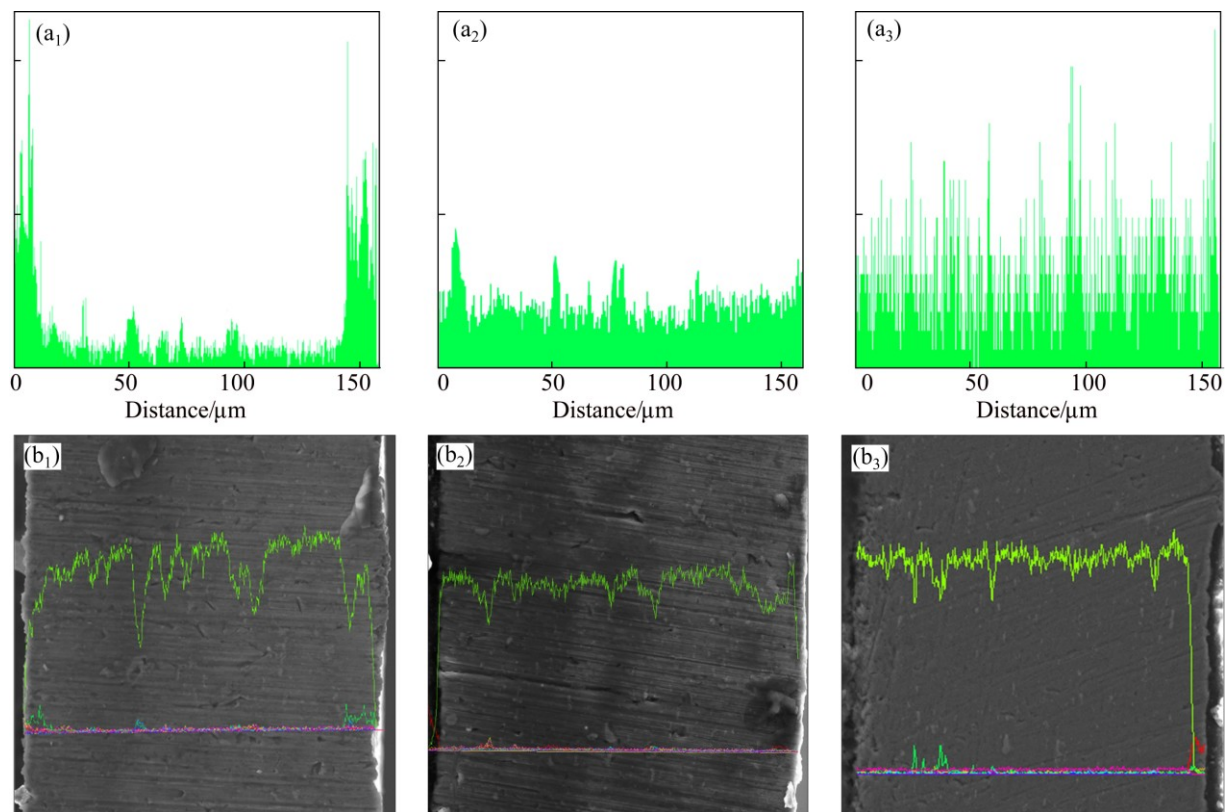


Fig. 9 Si element distribution across interface of 4343/3003/4343 clad sheet after sagging test: (a₁, b₁) Annealed at 380 °C for 1 h; (a₂, b₂) Annealed at 440 °C for 1 h; (a₃, b₃) Annealed at 550 °C for 1 h

Si diffusion rate. This has been corroborated by the near uniform Si distribution in Figs. 9(a₃) and (b₃). Therefore, with the rise of annealing temperature, the Si diffusion was accelerated, resulting in worsened sagging resistance.

During high temperature brazing, the melted clad layer penetrates into the core layer and develops coarse Al–Si eutectic phases at the intergranular. These Al–Si eutectic phases, completely melt during brazing, erode the grains in the core and reduce the effective core zone providing mechanical strength. As shown in Fig. 10, the extent of erosion in the core layer during brazing is positively correlated to the annealing temperature. For the specimen annealed at 380 °C, there is little erosion into the core during brazing, while the proportion of Al–Si penetrating depth ratio reaches 14.1% when annealing temperature increases to 550 °C. The deeper erosion area leads to the decrease of the effective core layer, which is in accordance with the weak sagging resistance.

4.3 Effect on sagging resistance with or without Si diffusion

To elucidate the effect of Si on sagging resistance, the sagging distances of both annealed 3003 core sheets without Si diffusion and 4343/3003/4343 clad sheets

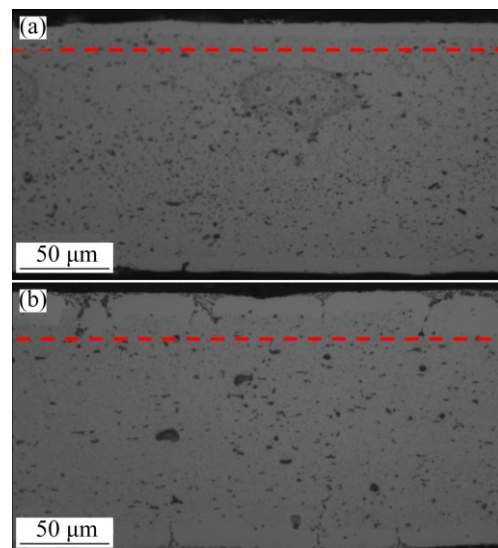


Fig. 10 Microstructures of 4343/3003/4343 clad sheet after sagging test: (a) Annealed at 380 °C for 1 h; (b) Annealed at 550 °C for 1 h, Al–Si penetrating depth ratio of 14.1%

with Si diffusion are listed in Table 3. As pointed out in Sections 4.1 and 4.2, the 4343/3003/4343 clad sheet annealed at 380 °C possesses the lowest sagging distance of 3.9 mm, with coarse grains and restricted Si diffusion. After higher temperature annealing, the grains in the

sheets become finer, and Si diffusion is accelerated, both of which will lead to much larger sagging distance.

After brazing, the grain size of the annealed clad sheet is nearly identical to that of the core sheet under the same annealing condition (in Table 2), which indicates similar microstructure as shown in Fig. 7. Therefore, the sagging distance of the core sheet can be deemed as the effect of microstructure. The difference of sagging distance between the core and clad sheets represents the effect of Si diffusion on the sagging resistance. At a brazing temperature below 380 °C, the difference is nearly constant and less than 4 mm. With the rise of annealing temperature, the difference increases rapidly and reaches 14.6 mm at 550 °C. Apparently, the Si diffusion will deteriorate the sagging resistance seriously as the annealing temperature grows. Moreover, the difference of sagging distance between the core and clad sheets under the same annealing process is much larger than the sagging distance of core sheet. It can be concluded that compared with the microstructure refinement, Si diffusion is the main factor that causes the annealed aluminum sheet to collapse during high temperature brazing.

Table 3 Sagging distances after brazing of annealed clad and core sheets

Annealing process	Sagging distance/mm		Difference between sagging distance of core sheet and clad sheet/mm
	Clad sheet	Core sheet	
Cold-rolled	8.3	4.7	3.6
280 °C for 1 h	6.8	3.1	3.7
380 °C for 1 h	3.9	0.5	3.4
440 °C for 1 h	9.5	3.8	5.7
500 °C for 1 h	15.7	5.6	10.1
550 °C for 1 h	22.9	8.9	14.6

5 Conclusions

1) With the increase of annealing temperature, the hardness values of both 4343/3003/4343 clad sheets and 3003 core sheets decrease significantly, indicating full recrystallization in the aluminum clad sheet. However, the sagging resistance is improved at first and then deteriorated with further increase of annealing temperature. The sheets annealed at 380 °C for 1 h possess the best sagging resistance.

2) In the 4343/3003/4343 clad sheet annealed at 380 °C for 1 h, the clad layer consists of fine and equiaxed recrystallized grains and the core layer is composed of fully recrystallized coarse grains elongated along the rolling direction. The coarse grain structure in the core layer reduces grain boundary slip, restrains the

Si penetration and improves sagging resistance during brazing. Further increasing the annealing temperature leads to abnormal grain refinement that facilitates the Si diffusion and weakens the sagging resistance.

3) Under the same annealing condition, the 3003 core sheet without Si diffusion has similar microstructure to that of 4343/3003/4343 clad sheet, but possesses distinctly better sagging resistance. Hence, the Si diffusion rather than the microstructure is the main factor affecting the sagging resistance.

References

- [1] MILLER W S, ZHUANG L, BOTTEMA J, WITTEBROOD A J, de SMET P, HASZLER A, VIIEGGE A. Recent development in aluminium alloys for the automotive industry [J]. *Materials Science and Engineering A*, 2000, 280: 37–49.
- [2] WITTEBROOD A J. Microstructural changes in brazing sheet due to solid–liquid interaction [M]. Delft: Delft University of Technology, 2009.
- [3] TURRIFF D M, CORBIN S F, KOZDRAS M. Diffusional solidification phenomena in clad aluminum automotive braze sheet [J]. *Acta Materialia*, 2010, 58: 1332–1341.
- [4] KARLÍK M, MÁNIK T, LAUSCHMANN H. Influence of Si and Fe on the distribution of intermetallic compounds in twin-roll cast Al–Mn–Zr alloys [J]. *Journal of Alloys and Compounds*, 2012, 515: 108–113.
- [5] HIRSCH J. Recent development in aluminium for automotive applications [J]. *Transactions of Nonferrous Metals Society of China*, 2014, 24: 1995–2002.
- [6] KAWAHARA A, NIKURA A, DOKO T. Development of aluminum alloy fin stock for heat exchangers using twin-roll continuous casting method [J]. *Furukawa Review*, 2003, 81–87.
- [7] GAO F, ZHAO H, SEKULIC D P, QIAN Y Y. Solid state Si diffusion and joint formation involving aluminum brazing sheet [J]. *Materials Science and Engineering A*, 2002, 337: 228–235.
- [8] RYU J S, KIM M S, JUNG D S. Brazeability of cold rolled three layer Al–7.5Si/Al–1.2Mn–2Zn–(0.04–1.0)Si/Al–7.5Si (wt.%) clad sheets [J]. *Journal of Materials Processing Technology*, 2002, 130–131: 240–244.
- [9] NOH S J, KIM M S, JUNG D, HAN J W, YOU B D. Effects of Si content and cold rolling condition on brazeability of Al–Mn–Zn alloy core brazing sheet [J]. *Materials Science Forum*, 2005, 486–487: 415–419.
- [10] QIN J N, KANG S B, CHO J H. Sagging mechanisms in the brazing of aluminum heat exchangers [J]. *Scripta Materialia*, 2013, 68: 941–944.
- [11] KIM S H, KANG J H, EUH K J, KIM H W. Grain-structure evolution of brazing-treated A4343/A3003/A4343 aluminum brazing sheets rolled with different reductions [J]. *Metals and Materials International*, 2015, 21: 276–285.
- [12] YOON J S, LEE S H, KIM M S. Sagging resistance of cold rolled aluminum 4343/3003/4343 clad sheet [J]. *Journal of Materials Science Letters*, 2001, 20: 229–232.
- [13] YOON J S, LEE S H, KIM M S. Fabrication and brazeability of a three-layer 4343/3003/4343 aluminum clad sheet by rolling [J]. *Journal of Materials Processing Technology*, 2001, 111: 85–89.
- [14] LEE S H, YOON J S, KIM M S, JUNG D. Effects of cold rolling parameters on sagging behavior for three layer Al–Si/Al–Mn(Zn)/Al–Si brazing sheets [J]. *Metals and Materials International*, 2002, 8: 227–232.
- [15] LEE S H, KIM M S, JUNG D S, HAN J W, YOU B D. Fabrication

- and sagging behavior of three-layer Al–Si/Al–Mn–Zn/Al–Si clad sheets for automotive heat exchanger [J]. *Materials Science Forum*, 2003, 439: 221–226.
- [16] POKOVÁ M, CIESLAR M, LACAZE J. The influence of silicon content on recrystallization of twin-roll cast aluminum alloys for heat exchangers [C]//Proceedings of the 12th International Symposium on Physics of Materials. Prague, 2012: 2625–2629.
- [17] SOMERDAY M, HUMPHREYS F J. Recrystallisation behaviour of supersaturated Al–Mn alloys Part 1: Al–1.3wt%Mn [J]. *Materials Science and Technology*, 2003, 19: 20–29.
- [18] TU Y Y, QIAN Huan, ZHOU Xue-feng, JIANG Jian-qing. Effect of scandium on the interaction of concurrent precipitation and recrystallization in commercial AA3003 aluminum alloy [J]. *Metallurgical and Materials Transactions A*, 2014, 45: 1883–1891.
- [19] JONES M J, HUMPHREYS F J. Interaction of recrystallization and precipitation: The effect of Al3Sc on the recrystallization behaviour of deformed aluminium [J]. *Acta Materialia*, 2003, 51: 2149–2159.
- [20] LIU W C, MORRIS J G. Evolution of recrystallization and recrystallization texture in continuous-cast AA 3015 aluminum alloy [J]. *Metallurgical and Materials Transactions A*, 2005, 36: 2829–2848.
- [21] WANG N, FLATØY J E, LI Y J, MARTHINSEN K. Evolution in microstructure and mechanical properties during back-annealing of AlMnFeSi alloy [J]. *Transactions of Nonferrous Metals Society of China*, 2012, 22: 1878–1883.
- [22] HUANG K, LI Y J, MARTHINSEN K. Isothermal annealing of cold-rolled Al–Mn–Fe–Si alloy with different microchemistry states [J]. *Transactions of Nonferrous Metals Society of China*, 2014, 24: 3840–3847.
- [23] TANGEN S, SJØLSTAD K, FURU T, NES E. Effect of concurrent precipitation on recrystallization and evolution of the P-texture component in a commercial Al–Mn alloy [J]. *Metallurgical and Materials Transactions A*, 2010, 41: 2970–2983.
- [24] HUANG K, LI Y J, MARTHINSEN K. Effect of heterogeneously distributed pre-existing dispersoids on the recrystallization behavior of a cold-rolled Al–Mn–Fe–Si alloy [J]. *Materials Characterization*, 2015, 102: 92–97.
- [25] HUMPHREYS F J, HATHERLY M. *Recrystallization and related annealing phenomena* [M]. 2nd ed. Amsterdam: Elsevier, 2004.
- [26] HUANG K, ENGLER O, LI Y J, MARTHINSEN K. Evolution in microstructure and properties during non-isothermal annealing of a cold-rolled Al–Mn–Fe–Si alloy with different microchemistry states [J]. *Materials Science and Engineering A*, 2015, 628: 216–229.
- [27] HUANG K, WANG N, LI Y J, MARTHINSEN K. The influence of microchemistry on the softening behaviour of two cold-rolled Al–Mn–Fe–Si alloys [J]. *Materials Science and Engineering A*, 2014, 601: 86–96.
- [28] TU Yi-you, TONG Zhen, JIANG Jian-qing. Effect of microstructure on diffusional solidification of 4343/3005/4343 multi-layer aluminum brazing sheet [J]. *Metallurgical and Materials Transactions A*, 2013, 44: 1760–1766.
- [29] SEKULIC D P, GALENKO P K, KRIVILYOV M D, WALKER L, GAO F. Dendritic growth in Al–Si alloys during brazing. Part 1: Experimental evidence and kinetics [J]. *International Journal of Heat and Mass Transfer*, 2005, 48: 2372–2384.
- [30] SUZUKI H, ITOH G, KOYAMA K. Deformation of brazing sheets affected by the structure of core materials during brazing [J]. *J Japan Inst Light Metals*, 1984, 34: 708–716.
- [31] LI Y J, ARNBERG L. Quantitative study on the precipitation behavior of dispersoids in DC-cast AA3003 alloy during heating and homogenization [J]. *Acta Materialia*, 2003, 51: 3415–3428.
- [32] HUANG H W, OU B L. Evolution of precipitation during different homogenization treatments in a 3003 aluminum alloy [J]. *Materials and Design*, 2009, 30: 2685–2692.
- [33] LI Y J, MUGGERUD A M F, OLSEN A, FURU T. Precipitation of partially coherent α -Al(Mn, Fe)Si dispersoids and their strengthening effect in AA 3003 alloy [J]. *Acta Materialia*, 2012, 60: 1004–1014.
- [34] CARLBERG T, JARADEH M, KAMAGA K H. Solidification studies of automotive heat exchanger materials [J]. *Aluminum Casting*, 2006, 58: 56–61.
- [35] LUDWIG W, PEREIRO-LÓPEZ E, BELLET D. In situ investigation of liquid Ga penetration in Al bicrystal grain boundaries: Grain boundary wetting or liquid metal embrittlement? [J]. *Acta Materialia*, 2005, 53: 151–162.

退火工艺对冷轧三层复合铝箔抗下垂性能的影响

赵媛媛, 章帧彦, 靳丽, 董杰

上海交通大学 轻合金精密成型国家工程研究中心和金属基复合材料国家重点实验室, 上海 200240

摘要: 采用硬度测试、EBSD 观察、EDS 分析及下垂试验系统地研究了退火工艺对冷轧 4343/3003/4343 复合铝箔及 3003 芯材铝箔的硬度、显微组织、Si 扩散及抗下垂性能的影响。研究表明, 随着退火温度的升高, 复合铝箔及芯材铝箔的硬度降低, 而两种铝箔均在 380 °C 退火 1 h 后获得最佳的抗下垂性能。380 °C 退火后, 复合铝箔的皮材组织为细小的等轴再结晶晶粒, 芯材由沿 RD 方向的粗大再结晶晶粒组成, 而皮材中少量 Si 向芯材扩散。在高温 440 °C 或 550 °C 退火后, 复合铝箔的抗下垂性能迅速恶化。其中皮材中晶粒长大, 导致皮材与芯材的界面变模糊; 芯材中的再结晶晶粒细化; 皮材中大量 Si 向芯材扩散。与高温退火后晶粒细化相比, 皮材向芯材的 Si 扩散是影响复合铝箔抗下垂性能的主要原因。

关键词: 铝合金; 显微组织; 退火; Si 扩散; 抗下垂性能

(Edited by Wei-ping CHEN)